Annals of the University of Craiova, Electrical Engineering series, No. 47, Issue 1, 2023; ISSN 1842-4805 eISSN 2971-9852

DOI: 10.52846/AUCEE.2023.01

On the Induction Motor Rotor Flux Estimation in the Electric Traction Systems with Rotor Flux-Oriented Control

Mihaela Popescu*, Alexandru Bitoleanu*, Constantin Vlad Suru* and Tudor Mătuşa*

* University of Craiova, Faculty of Electrical Engineering, Craiova, Romania, mpopescu@em.ucv.ro

Abstract - **Characterized by very good performance in both steady-state and dynamic regimes and also by a relatively simple control structure, the induction motor control with rotor flux orientation is frequently adopted in electric drive systems, especially in electric traction applications. This paper analyses the possibilities of rotor flux estimation in a real Romanian electric traction system of locomotives. Thus, to estimate the magnitude of rotor flux and the angular position of the rotor flux vector, two possibilities are identified and discussed. First, the use of the sensed speed and stator currents is taken into consideration, and then the use of the measured supply voltages and the stator currents is the second alternative. Dedicated algorithms were designed for their related control. Both variants are analyzed through the results of the simulations obtained based on the specific models created in the Matlab/Simulink software. Four values of the imposed speed are taken into account in the performed analysis. It is highlighted that, in real conditions where the drive system is provided with speed sensor and there is no sine filter for the distorted motor supply voltage, the best option to estimate the rotor flux is to use the measured speed and the stator currents.**

Cuvinte cheie: *motor asincon, control cu orientare după fluxul rotoric, estimarea fluxului rotoric, tracţiunea electrică a locomotivelor, controlul vitezei.*

Keywords: *induction motor, rotor flux-oriented control, rotor flux estimation, locomotives electric traction, speed control.*

I. Introduction

The field-oriented control method is one of the most used in the control of induction motors, ever since its proposal in the 1970s [1]. In short, to have good dynamic torque control as in the case of the direct current machine, the field-oriented control refers to the decoupling the torque and flux of the induction motor in a rotating reference frame. Clearly, the field-oriented control has much better performance compared to the classic V/f control [2]. The most common implementations consider the orientation according to the rotor flux. Using the components of the stator current in the rotating coordinates system (d, q) aligned with the rotor flux, the flux control is achieved by the d-axis current, whereas the torque control is achieved by the q-axis current. This control method is used in many applications, such as electric vehicles or traction applications [3]–[8].

To avoid using rotor flux sensors in the control scheme, the indirect control of the rotor flux is most often adopted, which involves the calculation of flux magnitude and its position starting from the operating equations of the induction motor, through model-based estimators [9]–[12].

There are many flux estimation approaches in the literature, some of which are based on the stator model, while others on the rotor model. For example, the Gopinath observer consists of two open-loop estimators, based on the stator or rotor models, depending on the speed range [13], [14]. An existing alternative in the literature is the use of non-linear observers, especially based on the sliding-mode theory [13], [15], [16]. One of the concerns is increasing the level of robustness in relation to disturbances and variation of the induction motor parameters.

In order to increase the performance of the control system, one of the researchers' concerns is taking into consideration phenomena such as the magnetic saturation, the dependence of motor parameters on temperature and the iron losses [14], [18], [19]. As an adaption method for the estimation of the rotor time constant, the online tuning of this constant is proposed in [18], by using the voltage model of the induction motor, which does not depend on rotor time constant, as the rotor flux reference model. In [19], based on the steady state model of the electrical drive, it is proposed to eliminate the rotor time constant from the control algorithm.

It must be clearly taken into account that the choice of the suitable method for estimating the rotor flux depends on the concrete application of the vector control. Specifically, the requirements regarding the required performance and the existing hardware resources lead to the choice of the appropriate method.

This paper analyses the possible options for estimating the rotor flux in the case of the electric locomotive traction system with induction motor and rotor flux-oriented control, equipped with speed sensor and without sine wave output filter at the inverter output.

This real system belongs to a Romanian company dealing with the modernization of locomotives.

The paper is organized as follows. Section II presents the possibilities of estimating the rotor flux in the physical system taken into consideration. Then, the performance of the rotor flux estimation approaches is analyzed based on modeling and simulation in the Matlab/Simulink environment for different imposed motor speeds. Finally, Section IV concludes this paper.

II. Possibilities of Estimating the Rotor Flux

To estimate the rotor flux in the real traction system taken into consideration, two possibilities were identified.

A. Estimation of the Rotor Flux Based on Speed and Stator Currents

When the rotor flux is estimated based on speed and stator currents, the block diagram in Fig. 1 highlights the speed control path followed by the active current (i_{sq}) control path. There is also the rotor flux control path followed by the reactive current (i_{sd}) control path. Each control path contains a controller of proportional–integral (PI) type, witch provide the prescribed values of the active current and reactive current respectively.

The gating signals for the power semiconductor devices are provided by a three-phase hysteresis band current controller designed to have a limited switching frequency [4].

Because three coordinate systems are used (three-phase (a, b, c), orthogonal stationary (α, β) and orthogonal rotating (d, q)), the transformation of quantities from one reference frame to another is performed through blocks BT_1, BT_2 and BT_3, that materialize specific transformation expressions [8], [20].

The calculation of the rotor flux magnitude Ψ_r and its angular position (λ) is done in the block Cψ, which has as inputs the components $i_{s\alpha}$ and $i_{s\beta}$ of the stator current vector and the sensed rotor speed (ω), as shown in Fig. 2. The following equations are involved [4], [8]:

$$\Psi_{r\alpha} = \int \left(-p\omega\Psi_{r\beta} - \frac{R_r}{L_r}\Psi_{r\alpha} + \frac{L_m R_r}{L_r}\mathrm{i}_{s\alpha}\right)dt; \quad (1)$$

$$\Psi_{r\beta} = \int \left(p\omega\Psi_{r\alpha} - \frac{R_r}{L_r}\Psi_{r\beta} + \frac{L_m R_r}{L_r}\mathrm{i}_{s\beta}\right)dt. \quad (2)$$

$$\Psi_r = \sqrt{\Psi_{r\alpha}^2 + \Psi_{r\beta}^2}. \quad (3)$$

$$cos\lambda = \frac{\Psi_{s\alpha}}{\Psi_r}; \qquad sin\lambda = \frac{\Psi_{s\beta}}{\Psi_r}. \quad (4)$$

In the above equations, ($\Psi_{r\alpha}$ $\Psi_{r\beta}$) are the components of the rotor flux vector in (α, β) reference frame; L_m is the magnetization inductance; R_r and L_r are the total phase rotor resistance and inductance referred to the stator; ω is the rotor speed; p is the number of pole pairs; λ is the position angle of the rotor flux vector with respect to the α-axis.

As illustrated in Fig. 2, the magnetization inductance is estimated based on magnetization characteristic. Also, the dependence of the rotor resistance as a function of temperature is considered. For this, it is approximated that the temperature of the rotor is equal to that of the stator, which is measured by a temperature sensor.

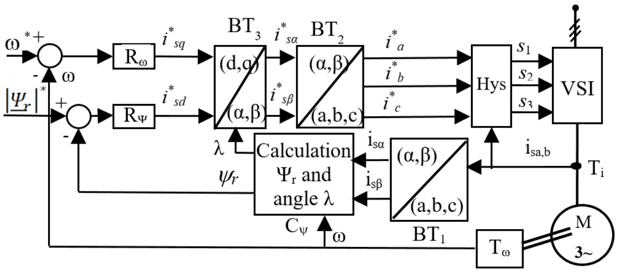

Fig. 1. Control block diagram of the induction motor, when the estimation of rotor flux is based on speed and stator currents.

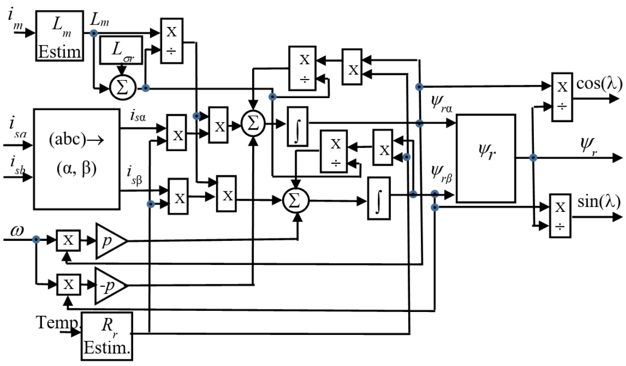

Fig. 2. The calculation of the rotor flux magnitude and its angular position based on speed and stator currents.

B. Estimation of the Rotor Flux Based on Voltages and Stator Currents

The associated control block diagram of the induction motor when the estimation of rotor flux is based on voltages and stator currents is shown in Fig. 3 and the specific structure of rotor flux calculation in Fig. 4 illustrates the following calculation expressions [8]:

$$\Psi_{s\alpha} = \int(v_{s\alpha} - R_s i_{s\alpha})dt; \quad (5)$$

$$\Psi_{s\beta} = \int\int(v_{s\beta} - R_s i_{s\beta})dt; \quad (6)$$

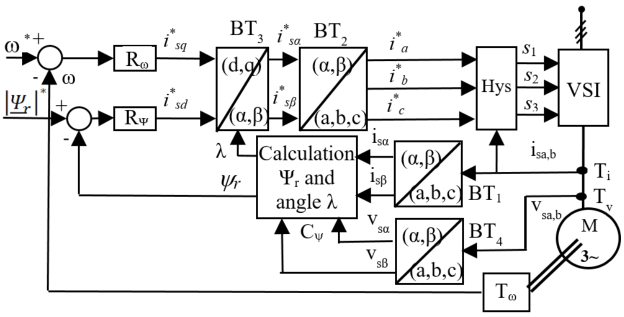

Fig. 3. Control block diagram of the induction motor, when the estimation of rotor flux is based on voltages and stator currents.

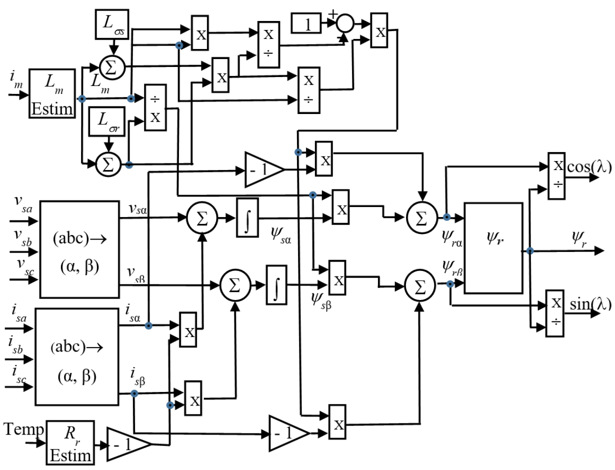

Fig. 4. The calculation of the rotor flux magnitude and its angular position based on voltages and stator currents.

$$\Psi_{r\alpha} = \Psi_{s\alpha}\frac{L_r}{L_m} - i_{s\alpha}\frac{L_s L_r}{L_m}\left(1 - \frac{L_m^2}{L_s L_r}\right); \qquad (7)$$

$$\Psi_{r\beta} = \Psi_{s\beta}\frac{L_r}{L_m} - i_{s\beta}\frac{L_s L_r}{L_m}\left(1 - \frac{L_m^2}{L_s L_r}\right). \qquad (8)$$

III. Performance of the Rotor Flux Estimation Approaches

In order to analyze the performance in the rotor flux-oriented control system applied in the field of electric traction of locomotives for the two flux estimation approaches, specific Simulink models were conceived and the simulation of the system operation at four imposed speeds was carried out. The main parameters of the real induction motor used in Romanian locomotives are summarized in Table I. It is noticed that the load torque taken into consideration has three components: a constant component; a component dependent on the speed; other component dependent on the square of the speed.

A. Case of Rotor Flux Estimation on the Basis of Speed and Stator Currents

1) Prescribed speed is 0.2 ω_N

In the case of low speed ramp prescription ($0.2\omega_N$), the response of the control system (Fig. 5) shows a very a very faithful tracking of the prescribed speed by the actual speed. The steady state error is very low (about 0.4%).

The time evolutions of the load and motor torques (Fig. 6) illustrate that, after the end of the transient regime, the motor torque is practically equal to the load torque. Fig. 7 highlights the evolution of the estimated rotor flux and its prescribed value. It can be seen that, in steady state regime, the two values of the flux are practical the same (about 2.488 Wb). The operation of the system with rotor flux orientation is confirmed by the zero value of the q-axis component of the rotor flux.

Also, as shown in Fig. 8, the sinusoidal waveforms of the rotor flux components in the stationary reference frame axes (α and β) confirm the correct operation of the system. The stator current components in the rotating reference frame (d, q) are very close to the prescribed values during the whole operation (Fig. 9).

TABLE I.
MAIN PARAMETERS OF THE INDUCTION MOTOR USED IN ROMANIAN LOCOMOTIVES

U_N (V)	P_N (kW)	f_{1N} (Hz)	p	I_N (A)	n_N (rpm)	T_N (N·m)
1400	1150	62.5	3	576	1237	8877
R_1 (Ω)	$L_{\sigma 1}$ (mH)	R_2 (Ω)	$L_{\sigma 2}$ (mH)	R_m (Ω)	L_{mN} (mH)	
0.021	0.288	0.012	0.275	89.38	9.46	

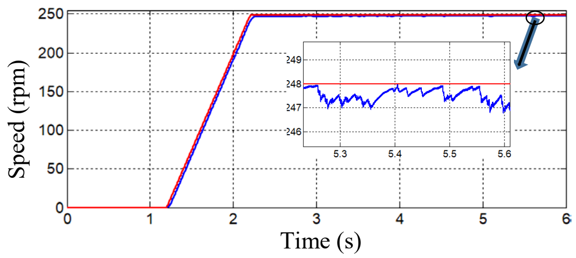

Fig. 5. Real speed (in blue) and prescribed speed (in red) in case of rotor flux estimation based on speed and stator currents, when $0.2\omega_N$ is prescribed.

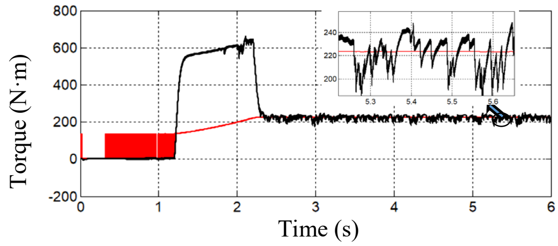

Fig. 6. Load torque (in red) and motor torque (in black) in case of rotor flux estimation based on speed and stator currents, when $0.2\omega_N$ is prescribed.

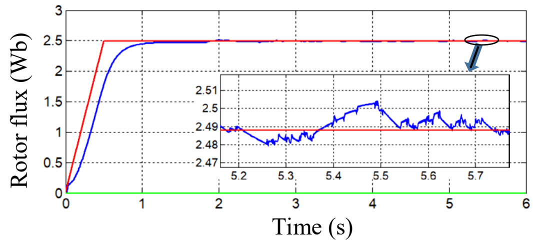

Fig. 7. Real rotor flux (in blue), prescribed rotor flux (in red) and q-axis component of the flux component (in green) in case of rotor flux estimation based on speed and stator currents, when $0.2\omega_N$ is prescribed.

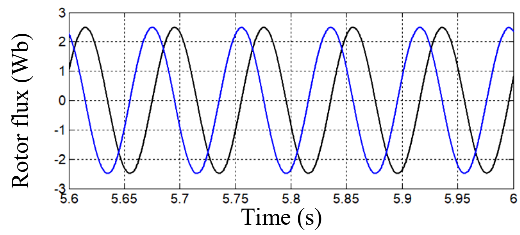

Fig. 8. α-axis component (in blue) and β-axis component of the rotor flux (in black) in case of rotor flux estimation based on speed and stator currents, when $0.2\omega_N$ is prescribed.

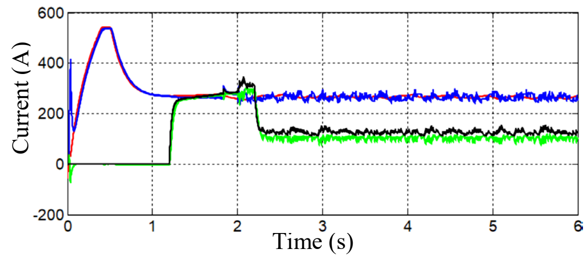

Fig. 9. Real i_{sd} (in blue); prescribed i_{sd} (in red); real i_{sq} (in green); prescribed i_{sq} (in black) in case of rotor flux estimation based on speed and stator currents, when $0.2\omega_N$ is prescribed.

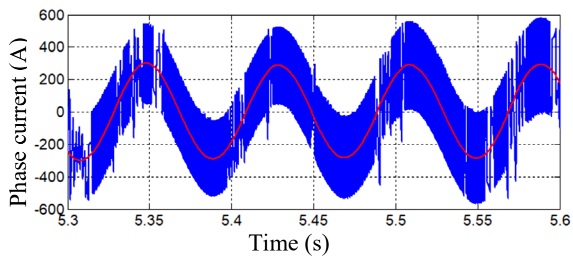

Fig. 10. Stator phase current (in blue) and its prescribed value (in red) in case of rotor flux estimation based on speed and stator currents, when $0.2\omega_N$ is prescribed.

Although it follows the sinusoidal evolution of the prescribed current, the stator current has a high degree of harmonic distortion at this low speed (Fig. 10).

2) Prescribed speed is 0.6ω_N

The second value of the prescribed speed taken into consideration is 740 rpm (about 0.6ω_N). First, the very good behavior of following the prescribed speed is highlighted (Fig. 11). The steady state error is below 0.14 %. The existence of a dynamic torque throughout the acceleration period followed by reaching the load torque are illustrated in Fig. 12. The prescribed rotor flux is also very well followed by the real one (Fig. 13). The components (prescribed and real) of the stator current in the rotating reference frame (d, q) are illustrated in Fig. 14. They are very close in values. As shown in Fig. 15, the phase stator current still has a high level of distortion, but lower than at the speed of 0.2ω_N.

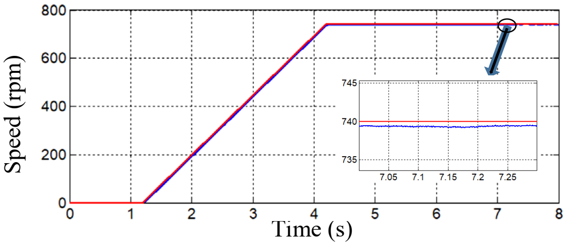

Fig. 11. Real speed (in blue) and prescribed speed (in red) in case of rotor flux estimation based on speed and stator currents, when 0.6ω_N is prescribed.

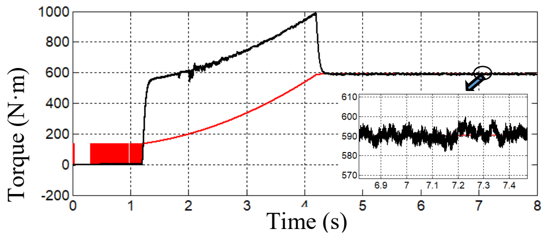

Fig. 12. Load torque (in red) and motor torque (in black) in case of rotor flux estimation based on speed and stator currents, when 0.6ω_N is prescribed.

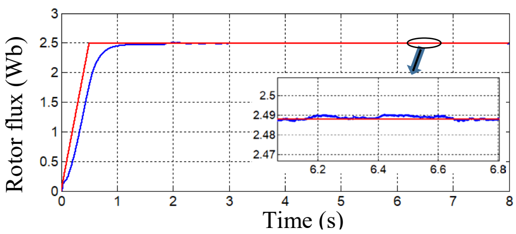

Fig. 13. Real rotor flux (in blue) and prescribed rotor flux (in red) in case of rotor flux estimation based on speed and stator currents, when 0.6ω_N is prescribed.

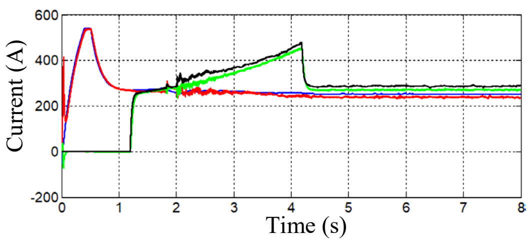

Fig. 14. Real i_{sd} (in blue); prescribed i_{sd} (in red); real i_{sq} (in green); prescribed i_{sq} (in black) in case of rotor flux estimation based on speed and stator currents, when 0.6ω_N is prescribed.

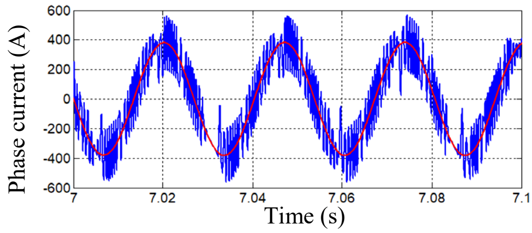

Fig. 15. Stator phase current (in blue) and its prescribed value (in red) in case of rotor flux estimation based on speed and stator currents, when 0.6ω_N is prescribed.

3) Prescribed speed is ω_N

When the nominal value of the speed (1237 rpm) is prescribed, it is also accurately followed (Fig. 16). The load and motor torques are practically equal in steady state operation, as shown in Fig. 17. It can be seen that the imposed rotor flux is very well followed (Fig. 18).

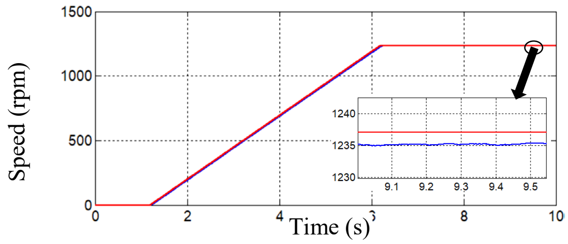

Fig. 16. Real speed (in blue) and prescribed speed (in red) in case of rotor flux estimation based on speed and stator currents, when ω_N is prescribed.

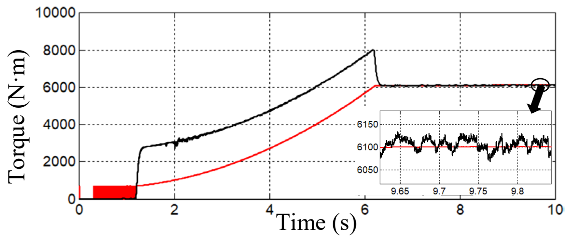

Fig. 17. Load torque (in red) and motor torque (in black) in case of rotor flux estimation based on speed and stator currents, when ω_N is prescribed.

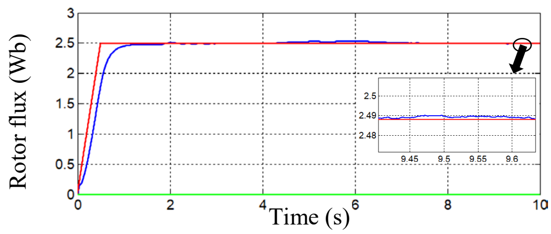

Fig. 18. Real rotor flux (in blue), prescribed rotor flux (in red) and q-axis component of the flux component (in green) in case of rotor flux estimation based on speed and stator currents, when ω_N is prescribed.

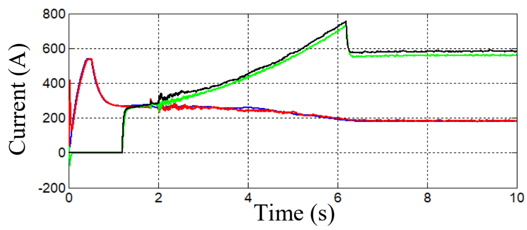

Fig. 19. Real i_{sd} (in blue); prescribed i_{sd} (in red); real i_{sq} (in green); prescribed i_{sq} (in black) in case of rotor flux estimation based on speed and stator currents, when ω_N is prescribed.

Fig. 19 shows the (d, q) stator current components and their prescribed values, which are very close to each other. As illustrated in Fig. 20, the magnetization inductance depends on the magnetization current. The stator current is closer to the prescribed value than at lower prescribed speeds (Fig. 21), with a lower total harmonic distortion factor (about 17%).

4) Prescribed speed is 1.6ω_N

The last value of the prescribed speed taken into consideration in the analysis is 1983 rpm (about 1.6ω_N). In this situation as well, the prescribed ramp speed is followed faithfully (Fig. 22). The equality between the torque developed by the induction motor and the load torque in steady state regime is very well illustrated in Fig. 23. At this high value of the prescribed speed, the prescribed rotor flux no longer has a constant value throughout the range of speed variation. It is 2.488 Wb when the speed is bellow the nominal value and then, it is reduced up to the value of 1.55 Wb, which is inversely proportional to the speed (Fig. 24). It can be seen that the real rotor flux accurately follows the prescribed value. The magnetization inductance evolution is shown in Fig. 25. The prescribed components of the stator current in the (d, q) reference frame are illustrated in Fig. 26 along with their real values, making evident very close values. From Fig. 27, it can be seen that the phase current is slightly more distorted than in the case of prescribing the nominal speed.

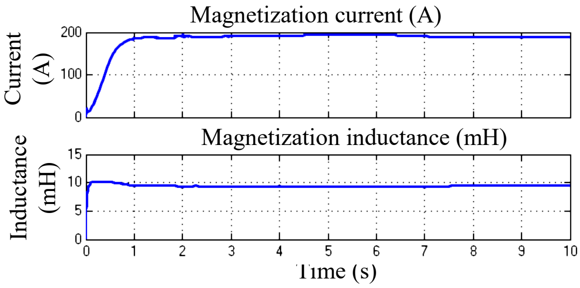

Fig. 20. Magnetization inductance in accordance with the magnetization current in case of rotor flux estimation based on speed and stator currents, when ω_N is prescribed.

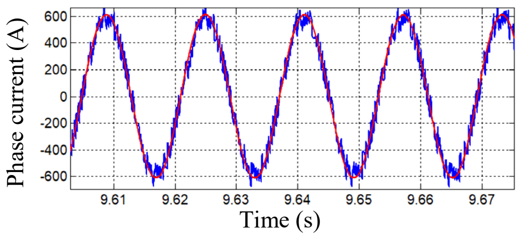

Fig. 21. Stator phase current (in blue) and its prescribed value (in red) in case of rotor flux estimation based on speed and stator currents, when ω_N is prescribed.

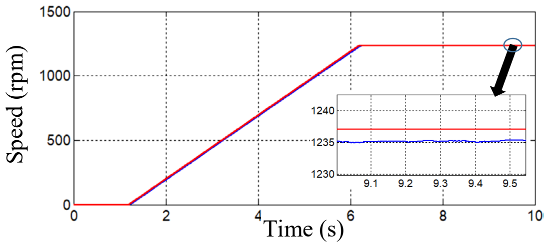

Fig. 22. Real speed (in blue) and prescribed speed (in red) in case of rotor flux estimation based on speed and stator currents, when 1.6ω_N is prescribed.

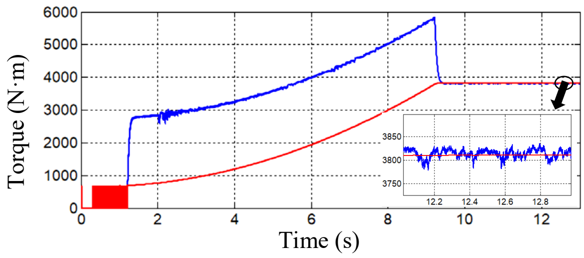

Fig. 23. Load torque (in red) and motor torque (in black) in case of rotor flux estimation based on speed and stator currents, when 1.6ω_N is prescribed.

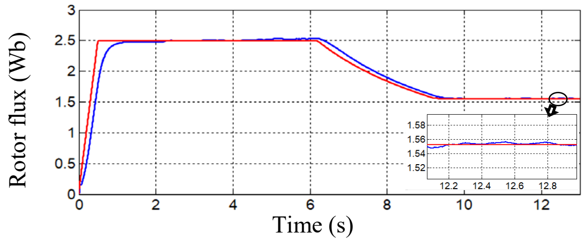

Fig. 24. Real rotor flux (in blue) and prescribed rotor flux (in red) in case of rotor flux estimation based on speed and stator currents, when 1.6ω_N is prescribed.

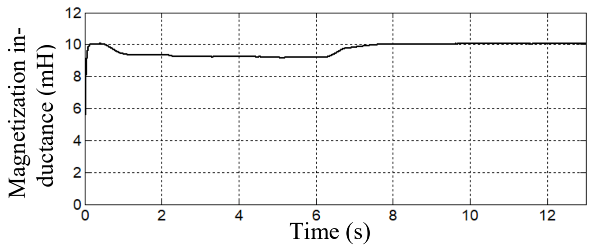

Fig. 25. The magnetization inductance evolution in case of rotor flux estimation based on speed and stator currents, when 1.6ω_N is prescribed.

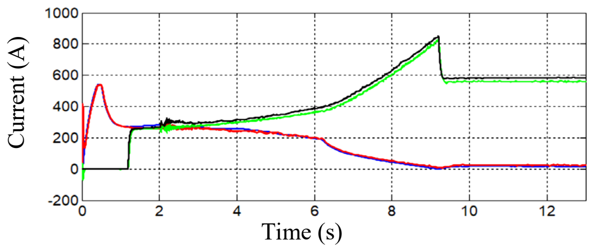

Fig. 26. Real i_{sd} (in blue); prescribed i_{sd} (in red); real i_{sq} (in green); prescribed i_{sq} (in black) in case of rotor flux estimation based on speed and stator currents, when 1.6ω_N is prescribed.

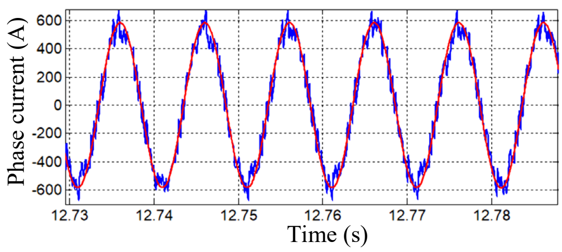

Fig. 27. Stator phase current (in blue) and its prescribed value (in red) in case of rotor flux estimation based on speed and stator currents, when 1.6ω_N is prescribed.

B. Case of Rotor Flux Estimation on the Basis of Voltages and Stator Currents

As stated previously, other possibility for estimation the rotor flux consists in using the measured voltages instead the measured speed.

It should be mentioned that this version faces difficulties in implementation because the voltage supplied by the inverter is much distorted and its precise measurement is not simple. Moreover, there is no voltage sensor in the physical system on which the proposed control will be implemented.

However, by simulation, for all the prescribed speeds taken into consideration, it is shown that the estimated rotor flux is very close to the one obtained in the case of rotor flux estimation on the basis of measured speed and stator currents. Fig. 28, Fig. 29, Fig. 30 and Fig. 31 illustrate the estimated rotor flux for the four prescribed speeds ($0.2\omega_N$, $0.6\omega_N$, ω_N and $1.6\omega_N$) compared with those estimated through the other method.

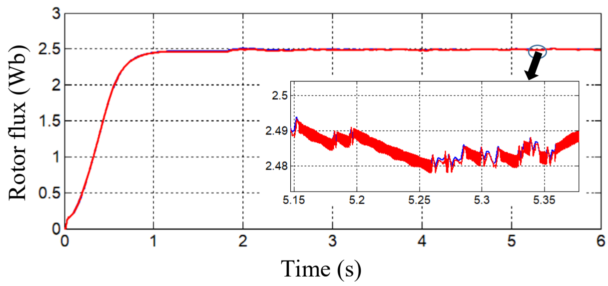

Fig. 28. Prescribed rotor flux in case of rotor flux estimation based on speed and stator currents (in blue) and in case of rotor flux estimation based on voltages and stator currents (in red), when $0.2\omega_N$ is prescribed.

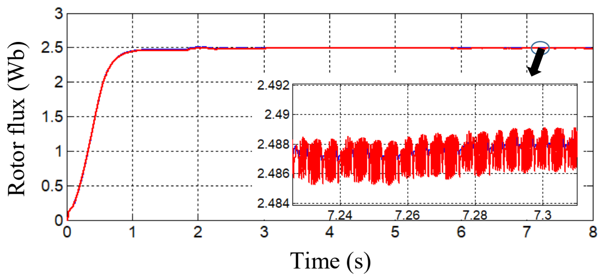

Fig. 29. Prescribed rotor flux in case of rotor flux estimation based on speed and stator currents (in blue) and in case of rotor flux estimation based on voltages and stator currents (in red), when 0.6ωN is prescribed.

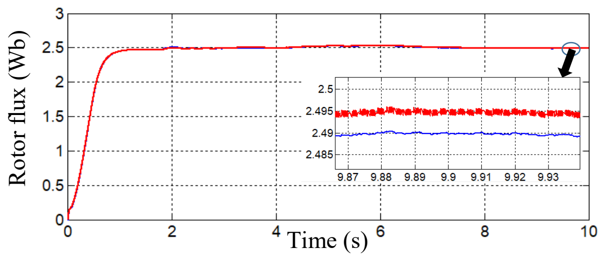

Fig. 30. Prescribed rotor flux in case of rotor flux estimation based on speed and stator currents (in blue) and in case of rotor flux estimation based on voltages and stator currents (in red), when ω_N is prescribed.

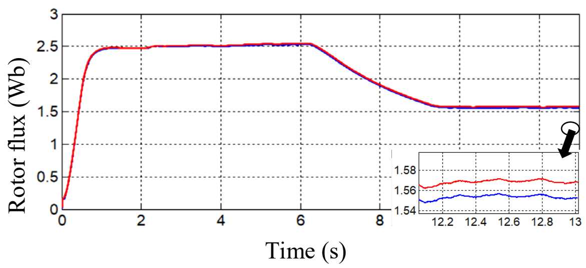

Fig. 31. Prescribed rotor flux in case of rotor flux estimation based on speed and stator currents (in blue) and in case of rotor flux estimation based on voltages and stator currents (in red), when $1.6\omega_N$ is prescribed.

If the values of the prescribed rotor flux calculated by the two methods are compared, it can be seen that, although they are very close, there are small oscillations of the prescribed flux in the case of rotor flux estimation based on voltages and stator currents, especially at low speeds (Fig. 28, Fig. 29, Fig. 30 and Fig. 31).

A possible alternative to measuring the distorted voltage could be its generation based on the inverter's IGBTs control signals.

When the waveforms of the measured and generated phase voltage are analyzed (Fig. 32), they appear to be identical at first glance.

Nevertheless, when the difference between the two-phase voltages is calculated, its time evolution (Fig. 33) shows that the phase voltage generated from IGBTs control signals is not very accurate.

As a natural consequence, the rotor flux estimated by using the calculated phase voltages from the control signals of the IGBTs is not acceptable, because it has large and unacceptable pulsations (Fig. 34).

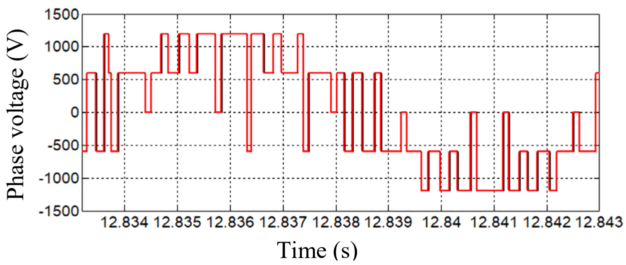

Fig. 32. Measured phase voltage (in red) and calculated phase voltage based on the control signals of the IGBTs (in black) when the prescribed speed is $1.6\omega_N$.

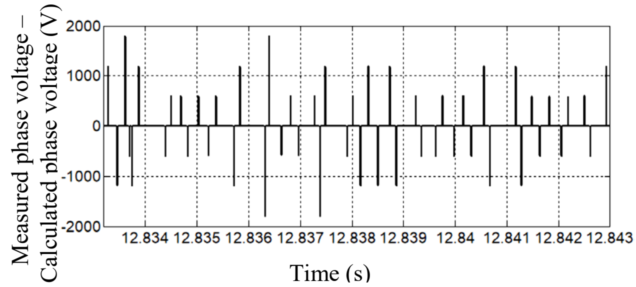

Fig. 33. Difference between the measured phase voltage and calculated phase voltage based on the e IGBTs' control signals when the prescribed speed is $1.6\omega_N$.

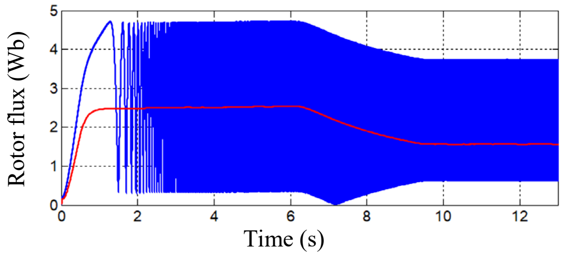

Fig. 34. Rotor flux (in blue) and its prescribed value (in red), when the rotor flux is estimated on the basis of the calculated phase voltage from the IGBTs' control signals and the prescribed speed is $1.6\omega_N$.

IV. Conclusions

From the analysis of the possibilities of estimating the rotor flux, it results that that use of the measured speed and stator currents leads to the best results, i.e. very good performance of the control system.

As a conclusion, it is the chosen method for rotor flux estimation, especially in the case of the induction motor used in the locomotive traction system on which vector control will be implemented.

The estimation of the rotor flux by using the IGBTs control signals is not a viable solution.

It is intended to implement the rotor flux-oriented control with rotor flux estimation based on the measured speed and stator currents for a railway traction motor in a Romanian company dealing with the modernization of locomotives.

Source of research funding in this article: Research program of the Department of Electromechanics, Environment and Applied Informatics, financed by the University of Craiova.

Contribution of authors:

First author – 50%

First coauthor – 20%

Second coauthor – 15%

Third coauthor – 15%

Received on October 29, 2023

Editorial Approval on November 30, 2023

References

[1] F. Blaschke, "A new method for the structural decoupling of ac induction machines," in *Conf.Rec.IFAC, Duesseldorf*, Germany, pp. 1-15, October 1971.

[2] S. Laha, J. Dhali and P. K. Gayen, "Comparative performance between V/F and rotor flux-oriented controls of induction motor drive," in *Proc. 2023 IEEE Devices for Integrated Circuit* (DevIC), Kalyani, India, 2023, pp. 1-6.

[3] L. Di Leonardo, M. Popescu, M. Tursini and M. Villani, "Finite elements model co-simulation of an induction motor drive for traction application," in *Proc. 45th Annual Conference of the IEEE Industrial Electronics Society* (IECON 2019), Lisbon, Portugal, 2019, pp. 1059-1065.

[4] M. Popescu, A. Bitoleanu and C.V. Suru, "Synthesis of rotor field-orientation control for induction traction motor," in *Proc.* 2021 *International Conference on Applied and Theoretical Electricity* (ICATE), Craiova, Romania, 2021, pp. 1-6.

[5] I. Zhurov, S. Bayda and S. Florentsev, "Field-oriented control of the induction motor as part of the shunting locomotive powertrain considering core losses and magnetic saturation," in *Proc. 29th International Workshop on Electric Drives: Advances in Power Electronics for Electric Drives* (IWED 2022), Moscow, Russian Federation, 2022, pp. 1-6.

[6] L. di Leonardo, M. Popescu, G. Fabri and M. Tursini, "Performance evaluation of an induction motor drive for traction application," in *Proc. 45th Annual Conference of the IEEE Industrial Electronics Soci*ety (IECON 2019), Lisbon, Portugal, 2019, pp. 4360-4365.

[7] M. Popescu, A. Bitoleanu and C. V. Suru, "Influence of locomotive wheels slipping on a traction system with rotor flux-oriented control and hysteresis current controllers," in *Proc. 2023 13th International Symposium on Advanced Topics in Electrical Engineering* (ATEE 2023), Bucharest, Romania, 2023, pp. 1-6.

[8] M. Popescu, A. Bitoleanu and C. V. Suru, "Estimation of the rotor flux in the traction systems with induction motors and field-oriented control," in *Proc. 14th International Conference and Exhibition on Electromechanical and Energy Systems* (SIELMEN 2023), Chișinău, Moldova, 12-13 October 2023, pp. 1-6.

[9] P. Mishra, R. Maheshwari and D. Patil, "Stabilization of rotor flux-oriented control of induction motor with filter by active damping," *IEEE Transactions on Industrial Electronics*, vol. 66, no. 12, pp. 9173-9183, Dec. 2019.

[10] I. Ferdiansyah, L. P. S. Raharja, D. S. Yanaratri and E. Purwanto, "Design of PID controllers for speed control of three phase induction motor based on direct-axis current (Id) coordinate using IFOC," in *Proc. 4th International Conference on Information Technology, Information Systems and Electrical Engineering* (ICITISEE), Yogyakarta, Indonesia, 2019, pp. 369-372.

[11] Y. Zidani, A. Boulmane and D. Belkhayat, "Improvement of the indirect field oriented control for IM drives using fuzzy controllers," in *Proc. 6th International Conference on Electrical and Electronics Engineering* (ICEEE), Istanbul, Turkey, 2019, pp. 45-49.

[12] V. V. Puranik, V. N. Gohokar, "Simulation of an indirect rotor flux oriented induction motor drive using Matlab/Simulink," *International Journal of Power Electronics and Drive System* (IJPEDS), vol. 8, no. 4, December 2017, pp. 1693~1704.

[13] O. Buchholz and J. Böcker, "Gopinath-observer for flux estimation of an induction machine drive system," in *Proc. 2017 IEEE Southern Power Electronics Conference* (SPEC), Puerto Varas, Chile, 2017, pp. 1-7.

[14] S. Dutta, A. Yoo, Y. Shi and V. C. Peddi, "A comparison of induction machine rotor flux observers in stationary reference frame for rotor flux position estimation," in *Proc. 2022 IEEE Energy Conversion Congress and Exposition* (ECCE), Detroit, MI, USA, 2022, pp. 1-8.

[15] X. Huihui, Z. Feng, C. Wei, and P. Wei, "Study of a new rotor flux estimator for induction machine based on sliding mode control," in *Proc. IEEE Vehicle Power and Propulsion Conference* (VPPC), Hangzhou, China, 2016.

[16] H. Xie, F. Wang, W. Zhang, C. Garcia, J. Rodríguez and R. Kennel, "Sliding mode flux observer based predictive field oriented control for induction machine drives," in *Proc. 2020 IEEE 9th International Power Electronics and Motion Control Conference* (IPEMC2020-ECCE Asia), Nanjing, China, 2020, pp. 3021-3025.

[17] X. Wu et al., "Improved rotor flux observer with disturbance rejection for sensorless SPMSM control," *IEEE Transactions on Transportation Electrification*, 2023.

[18] G. B. Reddy, G. Poddar and B. P. Muni, "Parameter estimation and online adaptation of rotor time constant for induction motor drive," *IEEE Transactions on Industry Applications*, vol. 58, no. 2, pp. 1416-1428, March-April 2022.

[19] H. Swami and A. Kumar Jain, "Reducing dependency on rotor time constant in a rotor flux oriented vector controlled induction motor drive based on its static model," in *Proc. 2022 IEEE Electrical Power and Energy Conference* (EPEC), Victoria, BC, Canada, 2022, pp. 430-437.

[20] B. Kimiaghalam, M. Rahmani and H. Halleh, "Speed & torque vector control of induction motors with Fuzzy Logic Controller," in *Proc. 2008 International Conference on Control, Automation and Systems*, Seoul, Korea (South), 2008, pp. 360-365.